Eur. J. Mineral.
2013, **25**, 519–531
Published online June 2013

Paper presented at the
European Mineralogical Conference,
emc^{2012}, Frankfurt/Main

Platinum-group minerals (PGM) nuggets from alluvial-eluvial placer deposits in the concentrically zoned mafic-ultramafic Uktus complex (Central Urals, Russia)

Federica ZACCARINI[1,*], Evgeny PUSHKAREV[2], Giorgio GARUTI[1], Joachim KRAUSE[3], Gennady p. DVORNIK[2,4],
Chris STANLEY[5] and Luca BINDI[6]

[1] Department Angewandte Geowissenschaften und Geophysik, Montan Universität, Peter Tunner Str. 5
8700, Leoben, Austria
*Corresponding author, e-mail: federica.zaccarini@unileoben.ac.at
[2] Institute of Geology and Geochemistry, Ural Division of Russian Academy of Sciences, Str. Pochtovy per. 7,
620151, Ekaterinburg, Russia
[3] Helmholtz Institute Freiberg for Resource Technology, Halsbrückes Str. 34, 09599 Freiberg, Germany
[4] Ural State Mining University, Str. Khokhryakova, Ekaterinburg, Russia
[5] Natural History Museum, Cromwell Road, London, SW7 5BD, UK
[6] Dipartimento di Scienze della Terra, Università di Firenze, Via La Pira 4 50121, Firenze, Italy

Abstract: We report the results of a detailed mineralogical investigation of platinum-group minerals (PGM) and copper-gold nuggets from the Uktus Ural-Alaskan type complex in the Central Urals (Russia). The studied nuggets were sampled in alluvial-eluvial deposits from three small valleys, with temporary water flows, cutting across the Uktus massif. The volume of the washed samples varies from 0.03 to 0.08 m^3 and a few tens of PGM nuggets, ranging in size from about 100 μm to about 2 mm, were collected. According to their chemical composition, the most abundant PGM are native Ir-Os and alloys in the Pt-Fe-Cu-Ni system. The following less abundant PGM were also recognised: sulfarsenides of the irarsite-hollingworthite-platariste series, sulfides such as laurite, cuproiridsite, kashinite and the sulfantimonide tolovkite. One alloy corresponding to the formula Cu_3Au_2 was found, and proved to be Cu-rich tetraauricupride. The nuggets of Uktus have, in some cases, a polygonal shape. However, most of them have an irregular morphology and are characterised by a porous rim and zoning. The investigated nuggets occur as single-phase crystals or as polyphase grains, composed of different PGM. One nugget displays a very complex texture, being composed of a Pt-Fe alloy associated with osmium and Cu-rich tetraauricupride. These minerals are in contact with quartz that contains minute inclusions of hollingworthite and platarsite. The mineralogical similarity with the PGM inclusions in the Uktus chromitites indicates these rocks as a possible source for the PGM nuggets. The presence of faceted morphology in some nuggets suggests that they were mechanically liberated and transported for a relatively short distance from their lode deposits. The nuggets characterized by a rounded shape and occurring in association with quartz and Cu-rich tetraauricupride have probably been reworked in the placer environment. Therefore, in the Uktus placers deposits, two types of PGM nuggets can coexist: (i) primary with a magmatic origin, *i.e.*, only mechanically liberated from their source rock, and (ii) secondary, *i.e.*, reworked and grown in the placers. The mineralogical assemblage of the Uktus PGM nuggets, the fact that the Uktus PGM placers have never been mined and the recent exponential increase in demand for noble metals make the placer deposits associated with the Uktus complex potentially important for the economic recovery of these rare metals, at least on a small scale.

Key-words: PGM nuggets, Cu-Au alloy, Uktus massif, Urals.

1. Introduction

The platinum-group elements (PGE) comprise six elements: Os, Ir, Ru, Rh, Pt and Pd. Due to their physical and chemical properties the PGE have gained, in the last decades, extremely high economic importance for their applications in many modern and advanced technologies, such as autocatalysts, and in the electrochemical and electronics industries. The PGE are also used in dental industry and they have important medical applications, such as chemotherapy. However, with an estimated concentration of about 10^{-6} to 10^{-7} % in the earth's crust, the PGE are numbered among the ultra-trace elements. For this reason, economic deposits of these metals are rare, and 90 % of the worldwide PGE production derives from a few mining districts in South Africa and Russia. Nowadays,

0935-1221/13/0025-2296 $ 5.85
DOI: 10.1127/0935-1221/2013/0025-2296
© 2013 E. Schweizerbart'sche Verlagsbuchhandlung, D-70176 Stuttgart

economic PGE deposits mainly occur associated with large igneous intrusions of the Bushveld type, and flood-basalts of the Siberian province (Cawthorn, 1999; Mudd, 2012). However, prior to the historical discovery of the Merensky Reef in the Bushveld complex (1927), for about one century (1824–1925) platinum was recovered from alluvial deposits of the Urals, which supplied more than 90 % of world platinum production. Since the beginning of the 20th century, it was established that platinum in placers of the Urals was derived from the erosion of dunites and chromitites in concentrically-zoned intrusions of the Uralian-Alaskan type (Duparc & Tikonowitch, 1920) that can host large crystals of PGM, such as those shown in Fig. 1. These complexes form the so-called Ural Platinum Belt, extending along the 60°E meridian between the 56°N and 64°N parallels, to the east of the Main Uralian fault in the Silurian-Devonian Tagil island-arc zone of the Ural orogen (Fig. 2A). It comprises a number of intrusive bodies (Fig. 2B), variable in size between approximately 50 and 700 km^2, emplaced at the root of the island arc during Paleozoic continental collision (Fershtater *et al.,* 1997). They are characterised by concentric zoning with a dunite core rimmed by wherlite, clinopyroxenite, gabbro and hornblendite (*e.g.* Garuti *et al.*, 2012a). The genesis of the Ural-Alaskan type complexes is related to magmatic activity in an island-arc setting associated with Paleozoic ocean-continent collision (Fershtater *et al.,* 1997). The first historical discovery of platinum nuggets in the Urals (1819, see Cabri & Genkin, 1991) took place in placers related to the erosion of a relatively small Ural-Alaskan type complex located in the proximity of the city of Ekaterinburg: the Uktus massif (Fig. 2B). Despite this significant discovery, the Uktus placers have never been mined and have been poorly investigated from a scientific point of view (Zaccarini *et al.,* 2007). The present study provides, for the first time, a detailed mineralogical description and composition of PGM collected in three different placers of the Uktus complex. Our goals are to compare the PGM found in the placers with those described in the Uktus chromitite lode deposits (Garuti *et al.,* 2002, 2003) and to discuss some genetic and economic aspects of the Uktus PGE mineralisation. Particular attention will be paid to the origin of the Uktus nuggets, taking into consideration the two major models proposed for the nuggets formation, *i.e*., (1) magmatic crystallisation within ultramafic intrusions, followed by their mechanical liberation and transport with no alteration prior to alluvial concentration (*e.g*. Cabri *et al.,* 1996) and (2) alteration of the PGM nuggets during weathering of the ultramafic source rocks, followed by the growth and reworking of PGM in the supergene environment (Fuchs & Rose, 1974; Bowles *et al.,* 2000; Talovina & Lazarenkov, 2001).

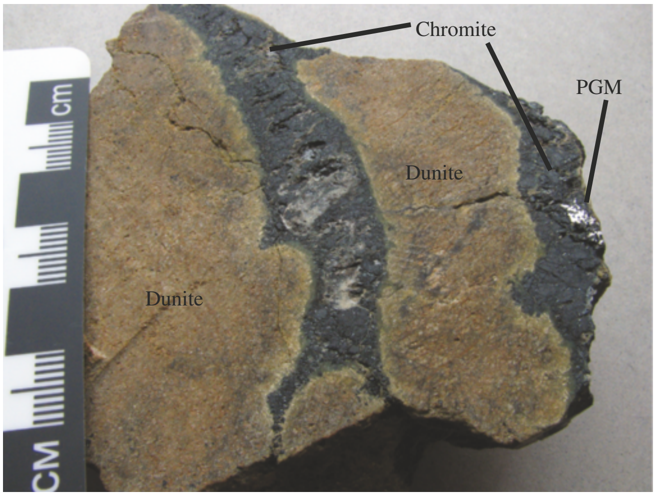

Fig. 1. Hand specimen of dunite and chromitite containing a coarse PGM grain from Niznhy Tagil complex.

2. Geological setting and location of the samples

The Uktus massif, covering an area of about 50 km^2, is one of the smallest Ural-Alaskan type complexes of the Urals. It is situated about 50 km to the east of the southern end of the Ural Platinum Belt, at the periphery of the city of Ekaterinburg (Fig. 2B). Although its location out of the Platinum Belt is anomalous, the Ural-Alaskan type affinity of the Uktus complex was established on the basis of petrographic and structural observations since the early 1920s (Tokarev, 1922). This conclusion was confirmed more recently by geochemical and petrographic data (Pushkarev & Puchkova, 1991; Pushkarev *et al.,* 1994, 1999; Pushkarev, 2000). The Uktus complex consists of dunite, clinopyroxenite, wherlite, olivine and amphibole gabbros, arranged in a concentrically zoned structure (Fig. 2C) in which dunite is rimmed by a wherlite-clinopyroxenite envelope, passing outwards into olivine and amphibole gabbros. The Uktus massif is in contact with an orogenic granite, Carboniferous in age, along the southern and eastern margins (Fig. 2C). However, no significant metamorphic effects caused by this granite intrusion are visible. The dunites are variably serpentinised (10–60 vol.%) and contain accessory chromite which locally forms small vermicular aggregates and minor chromitite lenses and layers, about 0.5–5 cm thick and 15–40 cm long. More extended lenses and pods up to some meters in size are rare and they occur only in the southern dunite body (Garuti *et al.,* 2003). The rocks of the Uktus massif crop out as a group of mounds rising up to 327–385 m above the surrounding lowland (∼250–300). Local topography shows three blocks (Northern, Central and Southern) separated by two main valleys running about W-E and SW-NE, respectively and corresponding to high-temperature plastic-shear zones dominated by gabbros. In contrast, the hilltops consist of ultramafic rocks (mainly dunite) and are elevated up to 40–60 m above the valley bottom. Each block is cut by numerous narrow, steeply sloping valleys, along with seasonal streams (mostly in springtime) flow intermittently. These valleys are floored with an eluvial-alluvial, poorly sorted deposit, from gravel to fine grained mud, of a few decimeters in thickness. During

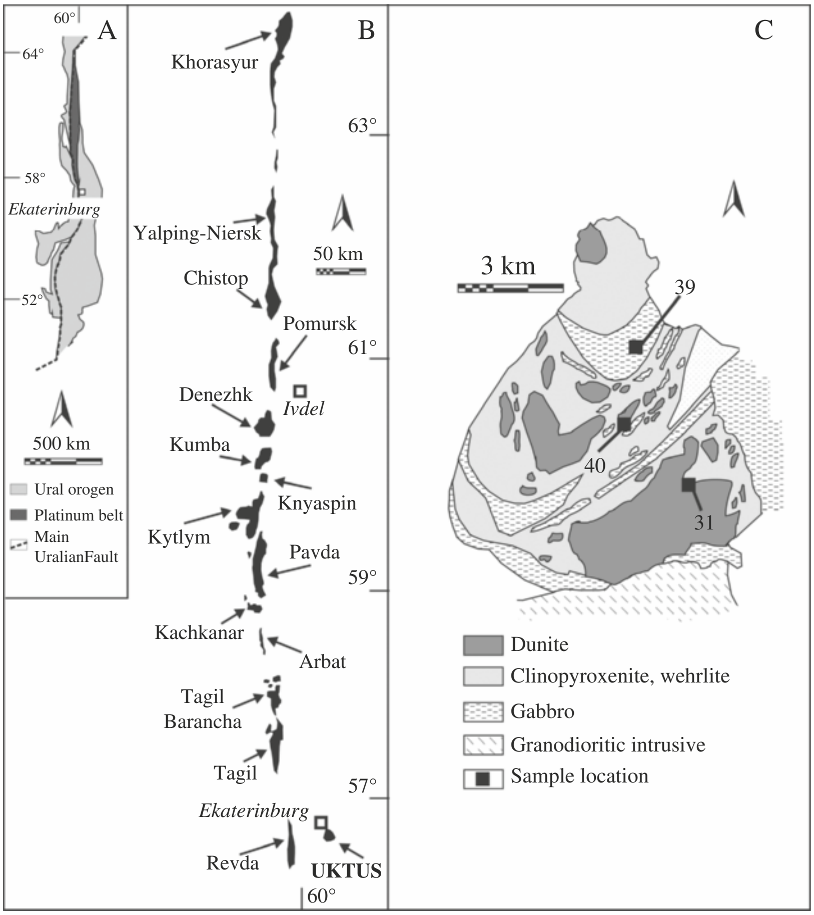

Fig. 2. (A) Geological setting of the Platinum bearing Belt in the Ural orogen. (B) Location of the major Ural Alaskan type complexes in the Ural Platinum bearing Belt (simplified after Yefimov *et al.,* 1993). (C) Geological map of the Uktus complex, showing the sample location (modified after Pushkarev *et al.,* 1999).

the Mesozoic (mainly in Triassic times) all of the ultramafic complexes of the Urals were deeply weathered, and several supergene deposits were formed. Weathering of the Uktus dunites produced a laterite cover up to several tens of meters thick that, at the locality of Elizavet in the central dunite body, was intensively exploited for Ni, Co and Mn extraction. Recent investigation (Talovina & Lazarenkov, 2001) proved that the supergene iron-rich rocks from the Elizavet deposit contain small grains of PGM (mainly Pd and Pt compounds) which differ from the PGM association established in the chromitite ores within dunite (Garuti *et al.,* 2003). The investigated nuggets were sampled in eluvial-alluvial deposits in three small valleys labelled 31, 39 and 40 (Fig. 2C). The volume of the washed samples varies from 0.03 to 0.08 m^3 and some tens of PGM nuggets were recovered.

3. Methodology

The morphology and size of the nuggets were investigated by scanning electron microscope at the University of Mainz (Germany) using a Jeol 8900 RL and at the Eugen F. Stumpfl laboratory (University of Leoben, Austria), using a Superprobe Jeol JXA 8200. The latter instrument, operating in WDS mode, was also used for quantitative analysis. Quantitative analysis was performed at 20 kV and 10 nA, using counting times as short as 20 and 10 s for peak and backgrounds, respectively. The beam diameter was about 1 μm. The nuggets were analyzed using pure metals as the reference material for PGE, electrum for Au and Ag, synthetic NiS, Pd_3HgTe_3 and PdSb and natural pyrite, chalcopyrite and niccolite for Fe, Ni, Cu, S, Sb, As and Hg. The X-ray lines used were: $K\alpha$ for S, Fe, Cu and Ni; $L\alpha$ for Ir, Ru, Rh, Pt, As and Sb; $M\alpha$ for Os. The following diffracting crystals were selected: PETJ for S, PETH for Ru, Os, Rh, Au, Ag, LIF for Cu, LIFH for Ni, Ir, Hg and Pt and TAP for As. Automatic corrections were performed for interferences involving Ru-Rh, Ir-Cu and Rh-Pd. The detection limits (wt.%) of the analyzed elements, automatically calculated by the microprobe software, are the following: As = 0.08, S = 0.01, Sb = 0.05, Ni = 0.04, Fe = 0.02, Cu = 0.05, Os = 0.08, Ir = 0.1, Ru = 0.02, Rh = 0.01, Pt = 0.1, Pd = 0.02, Au = 0.04, Ag = 0.03, Hg = 0.07. The same conditions were used to obtain the elemental distribution maps. Selected analyses of Uktus nuggets are presented in Tables 1 and 2. The compositions of very small grains included in large nuggets could be determined only qualitatively by EDS.

Table 1. Representative electron microprobe composition (wt%) of PGM from the Uktus nuggets.

PGM/sample		Os	Ir	Ru	Rh	Pt	Pd	Fe	Ni	Cu	S	As	Sb	Total
Iridium														
31/a 1 3		30.47	58.71	0.70	1.86	5.80	0.54	0.56	0.02	0.69	0.00	0.01	0.00	99.37
31/a 1 4		29.90	56.29	1.35	1.96	8.08	0.63	0.35	0.05	0.59	0.00	0.02	0.00	99.24
31/b 2a 2	Fig. 4A	26.13	57.66	3.04	1.72	8.73	0.62	0.34	0.04	0.73	0.00	0.08	0.00	99.09
31/b 2a 3	Fig. 4A	27.48	60.59	2.87	1.63	4.79	0.63	0.49	0.05	0.69	0.00	0.06	0.00	99.30
31/b 2a 4	Fig. 4A	36.29	56.07	0.79	0.13	0.00	0.11	4.08	0.30	0.78	0.19	0.05	0.00	98.79
31/b 1 2		20.31	67.17	3.56	1.42	6.08	0.60	0.29	0.07	0.67	0.04	0.16	0.00	100.37
31/b 1 10		20.33	66.88	2.66	1.57	5.84	0.58	0.80	0.14	0.79	0.00	0.22	0.00	99.79
31/b 1 11		44.58	50.34	0.71	0.43	0.00	0.15	0.89	0.11	0.60	0.20	0.52	0.00	98.54
31/b 4 1		35.36	58.20	1.63	0.83	1.62	0.30	0.14	0.04	0.61	0.00	0.02	0.00	98.76
31/b 4 2		32.89	60.52	1.75	0.81	2.45	0.39	0.29	0.07	0.58	0.00	0.10	0.00	99.84
31/c 1a 1		26.84	68.86	0.97	0.71	0.74	0.21	0.13	0.05	0.74	0.00	0.02	0.00	99.28
31 p1 2		26.36	58.31	2.63	1.50	7.96	0.50	0.37	0.06	1.12	0.00	0.05	0.00	98.86
31 p1 3		25.78	55.15	4.65	1.61	9.74	0.65	0.55	0.06	1.28	0.00	0.17	0.00	99.65
31 p1 5		25.83	57.53	3.94	1.62	10.12	0.65	0.83	0.06	1.01	0.00	0.12	0.00	101.71
31 p1 8		23.18	52.92	3.69	1.56	15.38	0.53	1.39	0.08	0.92	0.01	0.18	0.00	99.83
31 p1 9		24.43	54.35	4.12	1.46	12.39	0.60	0.96	0.04	0.97	0.04	0.15	0.00	99.51
31/4 p4 1	Fig. 5D	21.28	66.09	1.35	1.65	6.20	0.56	0.39	0.03	0.68	0.00	0.06	0.00	98.29
31/4 p4 6	Fig. 5D	21.19	67.00	1.50	1.75	5.94	0.55	0.46	0.00	0.78	0.00	0.05	0.00	99.23
31/7 p7 1		34.45	58.34	2.44	0.89	1.86	0.28	0.19	0.00	0.90	0.00	0.09	0.00	99.44
31/7 p7 2		34.29	58.40	2.15	0.87	2.61	0.36	0.13	0.02	0.86	0.00	0.08	0.00	99.77
31/9 p9 1		26.33	65.95	4.55	0.53	0.28	0.34	0.08	0.07	1.00	0.00	0.21	0.00	99.34
31/9 p9 2		25.88	66.96	4.61	0.64	0.22	0.30	0.12	0.02	0.84	0.02	0.19	0.00	99.78
31/9 p9 4		25.96	66.22	4.57	0.62	0.19	0.36	0.11	0.02	0.91	0.00	0.12	0.00	99.08
31/10 p10 1		30.84	59.68	2.20	1.45	3.78	0.48	0.24	0.03	0.70	0.00	0.07	0.00	99.47
31/10 p10 7		30.85	61.04	0.76	1.19	3.73	0.40	0.40	0.03	0.89	0.00	0.05	0.00	99.35
31/11 p11 1		21.64	68.34	2.07	1.12	3.85	0.31	0.28	0.06	1.59	0.01	0.12	0.00	99.38
31/11 p11 6		21.00	71.32	0.60	0.84	3.62	0.23	0.34	0.09	1.31	0.00	0.03	0.00	99.40
Osmium														
31/b 2b 1		56.58	39.05	3.36	0.55	0.00	0.24	0.06	0.00	0.47	0.00	0.11	0.00	100.42
31/b 2b 2		55.26	37.69	3.25	0.50	0.00	0.23	0.12	0.01	0.39	0.01	0.11	0.00	97.57
31/b 2b 3		55.39	37.82	3.57	0.40	0.00	0.30	0.08	0.00	0.52	0.02	0.10	0.00	98.20
31/b 3a 1	Fig. 4B	72.18	22.55	2.17	1.00	0.00	0.38	0.04	0.01	0.26	0.00	0.05	0.00	98.64
31/b 3a 2	Fig. 4B	71.05	22.98	2.96	0.91	0.00	0.34	0.08	0.01	0.30	0.00	0.14	0.00	98.78
31/b 3b 1		69.89	22.27	3.37	0.97	0.00	0.52	0.06	0.04	0.29	0.00	0.21	0.00	97.60
31/b 3b 2		69.37	23.22	3.14	1.09	0.00	0.48	0.04	0.06	0.30	0.03	0.09	0.00	97.83
40/1 1 1	Fig. 5A	72.08	24.77	0.56	1.33	0.00	0.49	0.01	0.00	0.38	0.04	0.07	0.00	99.71
31/8 p8 1		69.14	25.00	2.97	0.74	0.00	0.31	0.02	0.01	0.67	0.00	0.07	0.00	98.93
31/8 p8 2		71.57	21.89	2.62	0.71	0.00	0.32	0.10	0.04	0.68	0.00	0.12	0.00	98.05
31/8 p8 3		71.15	21.90	2.31	0.67	0.00	0.26	0.05	0.00	0.83	0.01	0.11	0.00	97.29
31/8 p8 4		72.41	21.86	2.26	0.68	0.00	0.26	0.06	0.04	0.38	0.00	0.11	0.00	98.06
31/8 p8 5		73.38	21.67	2.46	0.63	0.00	0.31	0.08	0.00	0.68	0.01	0.06	0.00	99.28
31/12 p12 8		66.97	6.18	4.28	0.86	14.83	0.41	2.84	0.66	2.12	0.00	0.19	0.00	99.35
Numbers 31 and 40 refers to the localities in Fig. 2.														
Pt-Fe alloys														
40/1 1 2	Fig. 5A	0.00	3.59	0.00	1.86	84.92	0.81	9.72	0.03	0.69	0.00	0.00	0.00	101.62
40/1 1 3	Fig. 5A	2.02	1.62	0.00	0.47	76.29	0.03	15.10	0.46	5.98	0.00	0.05	0.00	102.03
40/1 1 4	Fig. 5A	2.17	2.14	0.00	0.51	75.86	0.04	15.14	0.41	5.69	0.00	0.10	0.00	102.06
40/1 1 5	Fig. 5A	0.00	2.55	0.00	1.53	82.71	0.57	11.92	0.14	1.12	0.00	0.01	0.00	100.54
40/1 1 6	Fig. 5A	0.00	3.22	0.00	1.64	82.65	0.66	12.00	0.09	1.01	0.00	0.03	0.00	101.30
40/1 1 7	Fig. 5A	0.00	3.58	0.00	1.96	84.54	0.86	9.35	0.02	0.73	0.00	0.08	0.00	101.13
40/1 1 8	Fig. 5A	2.43	1.28	0.00	0.45	76.41	0.00	15.06	0.40	5.80	0.00	0.00	0.00	101.83
31/12 p12 9		3.07	0.00	0.00	0.36	74.62	0.03	12.28	3.20	7.16	0.00	0.00	0.00	100.73
31/12 p12 10		3.11	0.07	0.00	0.53	73.28	0.04	13.36	3.13	7.39	0.07	0.23	0.00	101.21
31/12 p12 12		3.46	0.45	0.00	0.70	71.27	0.09	11.85	2.92	7.67	0.32	0.65	0.00	99.38
Irarsite														
31/b 1 6		0.82	55.12	1.12	0.83	2.46	0.31	0.01	0.46	0.72	10.47	24.57	0.00	96.90
31/c 1b 1	Fig. 5C	3.65	49.72	1.07	0.88	3.52	0.35	0.00	1.05	0.53	11.19	25.32	0.00	97.27
31/c 1b 5	Fig. 5C	5.14	50.81	0.82	0.59	2.16	0.20	0.00	0.86	0.55	11.28	24.04	0.00	96.46
31/a 1 5		3.27	48.28	0.15	4.04	5.40	1.78	0.04	0.28	0.52	11.20	24.74	0.00	99.70
31/a 1 6		0.86	49.54	0.60	5.81	2.38	1.70	0.18	0.39	0.58	11.66	23.33	0.00	97.03

Table 1. Continued.

PGM/sample		Os	Ir	Ru	Rh	Pt	Pd	Fe	Ni	Cu	S	As	Sb	Total
31/13 p2 1	Fig. 5B	0.23	62.19	0.32	0.51	0.34	0.19	0.00	0.05	0.55	11.18	23.23	0.00	98.80
31/13 p2 2	Fig. 5B	0.00	61.26	0.58	0.66	1.13	0.24	0.01	0.09	0.63	10.89	23.54	0.00	99.03
31/13 p2 3	Fig. 5B	0.00	61.93	0.47	0.65	0.54	0.19	0.03	0.09	0.56	10.71	23.80	0.00	98.99
31/13 p2 4	Fig. 5B	0.66	61.85	0.33	0.40	0.17	0.15	0.00	0.10	0.64	10.20	24.37	0.00	98.88
31/13 p2 5	Fig. 5B	0.00	59.32	0.69	0.92	1.20	0.25	0.00	0.01	0.62	11.39	23.72	0.00	98.13
31/13 p2 6	Fig. 5B	0.05	60.71	0.42	0.58	0.23	0.18	0.00	0.10	0.59	11.00	22.66	0.00	96.52
31/13 p2 7	Fig. 5B	0.00	57.50	0.73	0.89	1.60	0.28	0.02	0.08	0.64	9.96	24.73	0.00	96.43
unknown Ir-Os sulfarsenides														
31/b 1 7		12.85	58.77	1.18	0.47	1.05	0.20	0.37	0.13	0.78	7.13	12.61	0.00	95.54
31/c 1b 3	Fig. 5C	31.82	47.67	0.77	0.00	0.00	0.03	0.77	0.20	0.53	3.64	9.55	0.00	94.98
31/c 1b 6	Fig. 5C	17.84	49.34	0.55	0.20	0.00	0.11	0.07	0.16	0.54	8.18	18.72	0.00	95.71
31/c 1b 4	Fig. 5C	29.66	47.26	0.83	0.03	0.36	0.06	0.19	0.21	0.60	4.76	11.93	0.00	95.90
Tolovkite														
31/c 1b 2rip	Fig. 5C	0.00	53.82	0.00	1.00	0.26	0.45	0.02	0.07	0.50	9.78	1.27	34.05	101.21
31/c 1b 8 rip	Fig. 5C	0.00	54.27	0.04	0.59	0.15	0.34	0.09	0.05	0.57	9.81	1.17	35.62	102.69
31/c 1b 7 rip	Fig. 5C	0.00	50.30	0.09	1.46	0.43	0.80	0.03	0.12	0.65	9.12	2.71	30.96	96.66

Table 2. Composition of the Au-Cu alloy of the Uktus nugget.

Wt%	Cu	Ag	Au	Fe	Pd	Sb	Total
40g14an1	33.79	0.23	65.21	0.02	0.35	0.18	99.78
40g14an2	33.63	0.23	64.22	0.06	0.30	0.21	98.64
40g14an3	32.38	0.27	67.10	0.01	0.32	0.16	100.23
40g14an4	33.53	0.23	65.65	0.04	0.25	0.19	99.88
40g14an5	33.27	0.27	64.61	0.06	0.31	0.24	98.77
At%	Cu	Ag	Au	Fe	Pd	Sb	
40g14an1	61.10	0.25	38.06	0.05	0.37	0.17	
40g14an2	61.32	0.24	37.79	0.12	0.32	0.20	
40g14an3	59.43	0.29	39.76	0.02	0.35	0.15	
40g14an4	60.80	0.24	38.42	0.09	0.27	0.18	
40g14an5	60.86	0.30	38.15	0.12	0.34	0.23	
a.p.f.u.	Cu	Ag	Au	Fe	Pd	Sb	
40g14an1	3.06	0.01	1.90	0.00	0.02	0.01	
40g14an2	3.07	0.01	1.89	0.01	0.02	0.01	
40g14an3	2.97	0.01	1.99	0.00	0.02	0.01	
40g14an4	3.04	0.01	1.92	0.00	0.01	0.01	
40g14an5	3.04	0.01	1.91	0.01	0.02	0.01	

A small crystal fragment (35 × 40 × 50 μm) of Cu-Au alloy, dug out from a polished thin section, was selected for the X-ray single-crystal diffraction study. Tetragonal unit-cell parameters, determined by centering 25 high-θ (16–22°) reflections on an automated diffractometer (Bruker MACH3), are $a = 3.909(1)$, $c = 3.621(1)$ Å, and $V = 55.33(8)$ Å^3. To check the possible presence of diffuse scattering or weak superlattice peaks, the crystal was also mounted (exposure time of 200 s per frame; 40 mA × 40 kV) on a CCD-equipped diffractometer (Oxford Xcalibur^{TM} 3), but no additional reflections were detected.

4. The PGE nuggets of Uktus

4.1. Morphology and mineralogy

The nuggets of Uktus have a size variable from about 100 μm up to about 2 mm. An external polygonal shape has been observed in some cases (Fig. 3A, B), however, most of the nuggets have an irregular morphology and are characterised by internal zoning, sometimes with concentric symmetry, manifested by variations in electronic reflectance, and porous rims.

According to chemical determination, the most abundant PGM are iridium, osmium (localities 31 and 39, Fig. 2C), and subordinate Pt-Fe alloys (locality 40, Fig. 2C). One alloy containing Cu and Au as the major constituents was also encountered at locality 40. Sulfarsenides of the irarsite–hollingworthite–platarsite series are common. Irarsite frequently occurs as a major constituent of composite nuggets (Fig. 5B, C), whereas hollingworthite and platarsite only form minute inclusions and, therefore, were only qualitatively identified. Other accessory PGE phases (laurite, cuproiridsite, kashinite, tolovkite) were found as minor constituents of iridium nuggets. The PGM sulfides were only qualitatively identified, and quantitative

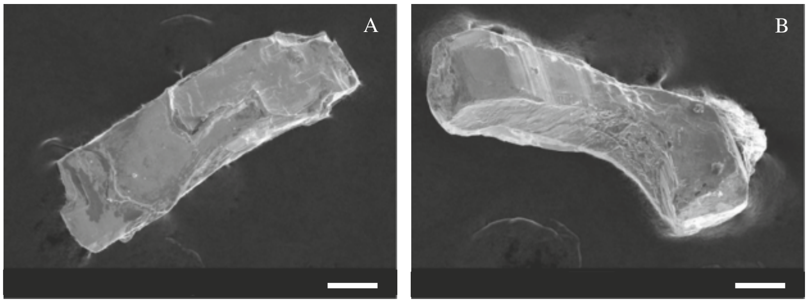

Fig. 3. Secondary electron image of the Uktus PGM nuggets, showing their polygonal shape. Scale bar = 50 μm.

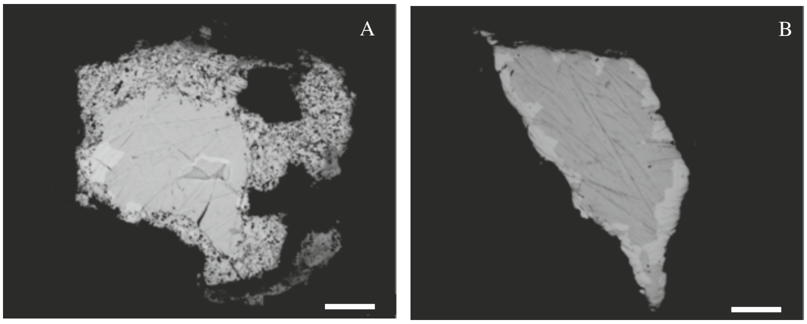

Fig. 4. Back-scattered electron images (BSE) of Os-Ir nuggets from Uktus: (A) chemically zoned iridium, more reflectant zones are Pt-rich, less reflectant Ru-rich, the porous rim contains Fe; (B) chemically zoned osmium, more reflectant rims have slightly higher Ir/Os ratio. Scale bar = 50 μm.

analysis could be obtained for tolovkite only. The nuggets may consist of a single phase, although showing chemical zoning (Fig. 4A, B), or form polyphase aggregates, composed of different PGM. The BSE images obtained during this work show different types of assemblages. The composite nugget in Fig. 5A consists of two Pt-Fe alloys characterised by different electronic reflectance. One occurs at the core of the nugget and is associated with

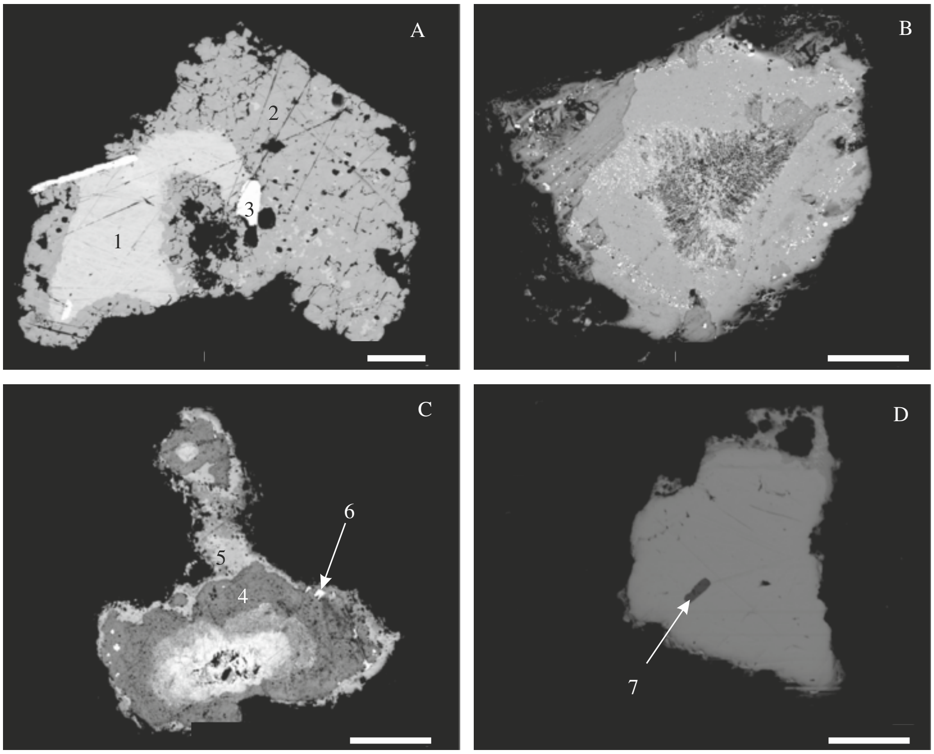

Fig. 5. BSE images of Uktus nuggets: (A) Pt-Fe alloy (1), Cu-rich tetraferroplatinum (3) and osmium (4), (B) irarsite with blebs of osmium (white), (C) zoned irarsite (4) rimmed by tolovkite (5) with spots of osmium (6), (D) iridium with an inclusion of laurite (7). Scale bar = 50 μm.

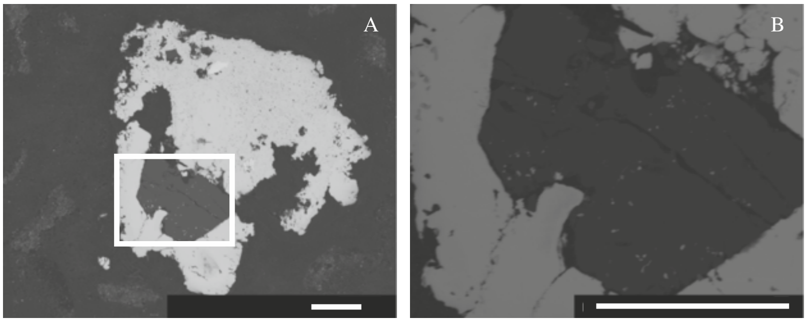

Fig. 6. BSE images of Uktus PGM nugget composed of (A) Pt-Fe alloy, Cu_3Au_2 and osmium, (B) enlargement of (A) showing an inclusion of quartz containing small spot of irarsite and hollingworthite. Scale bar = 50 μm.

three osmium lamellae, the other forms the external body of the nugget and is porous and fractured. Two nuggets mainly composed of irarsite show different zoning. One consists of irarsite minutely spotted with native osmium (Fig. 5B), the other shows a cockade-like texture consisting of a bright core of unidentified Ir-Os sulfarsenides surrounded by irarsite rimmed by tolovkite and small spots of native osmium (Fig. 5C). Laurite as well as other PGE sulfides may occur as minute inclusions in iridium (Fig. 5D). The Cu-Au alloy is part of a polyphase nugget also containing a Pt-Fe alloy minutely spotted with Cu-Au, Ir-Rh-Pt sulfarsenides and native osmium (Fig. 6A). The core of the nugget consists of quartz that contains minute blebs of hollingworthite and platarsite (Fig. 6B). Due to their small size, the sulfarsenide inclusions were identified by EDS analyses. The complex intergrowth of this nugget is shown in the X-ray element-distribution map of Fig. 7.

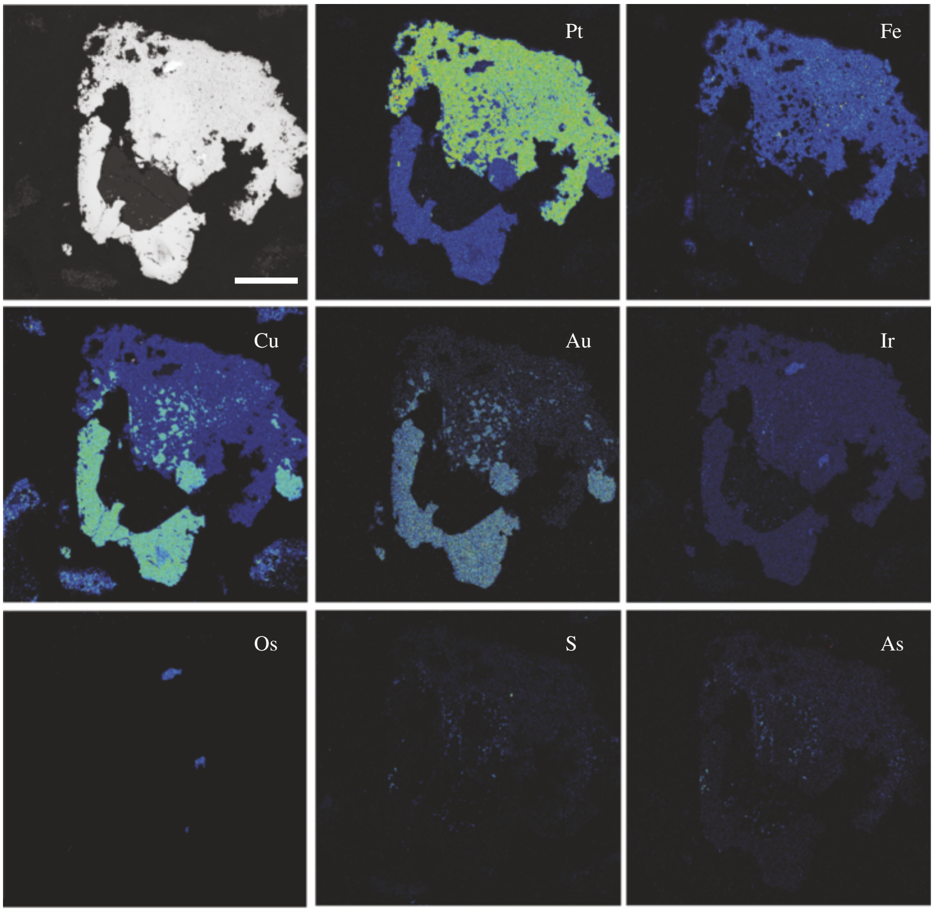

Fig. 7. BSE image and X-ray element-distribution maps of Pt, Fe, Cu, Au, Ir, Os, S, As, showing the complex mineral assemblage of the nugget of Fig. 6. Scale bar = 50 μm.

4.2. Mineral chemistry

4.2.1. Iridium and osmium

The compositions of iridium and osmium, as atomic proportions, have been plotted in the Os-Ir-Ru triangle and compared with the analyses reported by Garuti *et al.* (2002, 2003) for similar alloys found included in the Uktus chromitites (Fig. 8). Iridium contains substantial amounts of Os (18.7–42.7 atom %), with an Ir/Os atomic ratio varying from 3.40 to 1.12. It also contains Ru from 1.3 to 6.6 atom %, Rh up to 3.5 atom %, and Pt up to 12.6 atom %. Reciprocal variations in Ir/Os ratio, Pt, Ru, and the sporadic appearance of Fe (up to 12.4 atom %) and Cu (up to 2.4 atom %) account for the observed changes in electronic reflectance (Fig. 4A). Generally, osmium contains Ir from 21.0 to 36.8 atom %, with Os/Ir atomic ratios between 3.42 and 1.46, and Ru from 1.02 to 6.5 atom %. Several grains are chemically zoned showing decrease of the Os/Ir atomic ratio along rims (Fig. 4B). Only one grain of osmium, characterised by extremely high Os/Ir atomic ratio (10.95), was found to contain 12.4 atom % Pt.

4.2.2. Pt-Fe alloys

The compositions of the Pt-Fe alloys from the Uktus nuggets were plotted, as atomic proportions, in the Pt-Fe-(Cu + Ni) ternary diagram (Fig. 9) and compared with data from Pt-Fe alloys in the Uktus chromitites (Garuti *et al.,* 2002, 2003). Some alloys forming the solid core of nuggets contain Os lamellae (Fig. 5A) and have isoferroplatinum-type stoichiometry ($Pt_{3-x}Fe$) with minor amounts of Ir (2.8 atom %), Rh (2.9 atom %), Pd (1.2 atom %) and Cu (1.7 atom %). They closely compare with alloys occurring as primary magmatic inclusions in the Uktus chromitites (Fig. 9). The fractured and porous alloy forming the external part of the nugget (Fig. 5A) approaches the composition of tetraferroplatinum (PtFe) with up to 1.4 atom % Os and Ir, substituting for Pt. The porous alloy is spotted with minute particles of a Pt phase having stoichiometry Pt_2 (Fe > Cu) intermediate between isoferroplatinum and tetraferroplatinum. The Pt-Fe alloy associated with the Cu-Au alloy approaches the Pt_2CuFe stoichiometry of tulameenite, with remarkable substitution of Os (5.7 atom %) and Ni (6.9 atom %) for Pt and Cu, respectively.

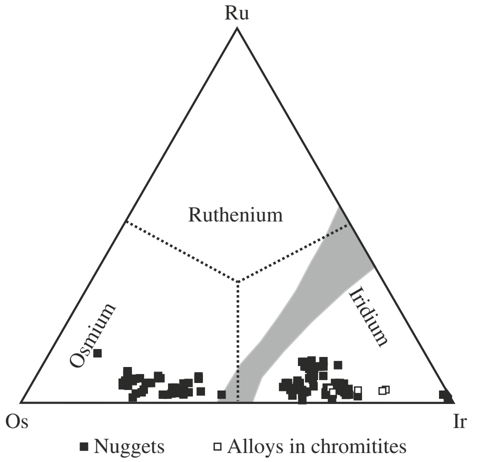

Fig. 8. Compositions (atom %) of Os–Ir–Ru alloys from Uktus nuggets (black square, present work) and from Uktus chromitites (white square), data from Garuti *et al.*, (2002, 2003). The field of the miscibility gap (Harris & Cabri, 1973) is shown in grey.

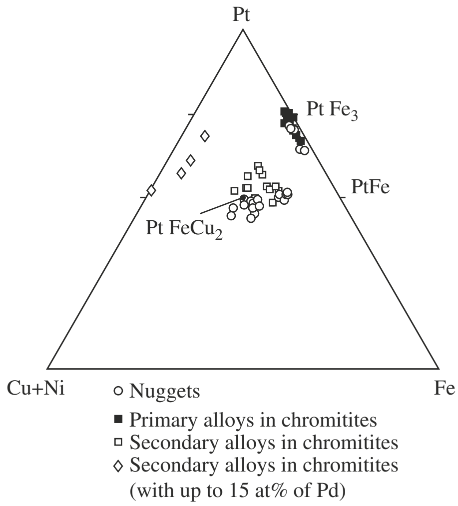

Fig. 9. Compositions (atom %) of Pt alloys from Uktus nuggets (present work) and from Uktus chromitites (Garuti *et al.,* 2002, 2003).

The Pt-Fe alloys with tetraferroplatinum- and tulameenite-type composition are similar to the Pt-Fe alloys analyzed in the Uktus chromitites (Fig. 9) and classified as secondary phases (Garuti *et al.,* 2002, 2003).

4.2.3. Irarsite, unknown Ir-Os sulfarsenide, and tolovkite

The compositions obtained from four different nuggets show appreciable amounts of Rh (up to 5.4 atom %), Pt (up to 2.6 atom %), Os (up to 2.7 atom %), Pd (up to 1.6 atom %), Ru (up to 1.2 atom %), Ni (up to 1.7 atom %), and Cu (up to 1.1 atom %) substituting for Ir. The compositions reflect the theoretical stoichiometry IrAsS, with average Ir/(S + As) and S/As atomic ratios of 0.53 and 1.07, respectively, thus indicating slight excess of metal and sulfur. The Ir-Os sulfarsenide, forming the core of the zoned nugget in Fig. 5C, is compositionally heterogeneous showing variable amounts of Os from 8.4 to 24.3 atom %, substituting for Ir, and minor amounts of Ru (0.6–1.4 atom %), Fe (0.0–2.0 atom %), and Cu (0.56–1.5 atom %). The calculated stoichiometry reflects (Ir + Os)/(S + As) and S/As atomic ratios varying in the ranges 0.74–1.86 and 0.93–1.32, respectively. The compositions of irarsite and the unknown Ir-Os sulfarsenide were plotted as atomic proportions in the Ir-Os-Rh triangle of Fig. 10.

Tolovkite from the nugget in Fig. 5C well corresponds well to the theoretical formula IrSbS, although it shows small amounts of Rh (0.63–1.62 atom %) and Cu (0.87–1.17 atom %) substituting for Ir, and As (1.7–4.1 atom %) replacing Sb.

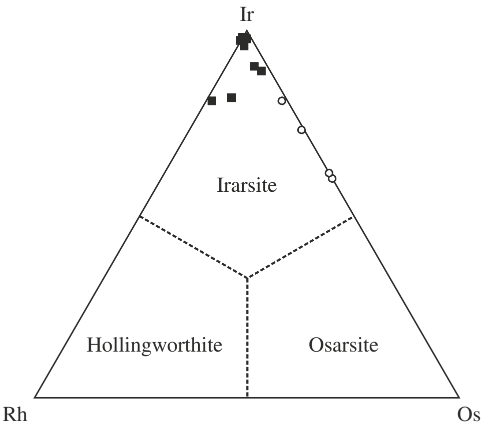

Fig. 10. Compositions (atom %) of irarsite (black square) and Ir-Os sulfarsenides (open circle) from Uktus nuggets.

4.2.4. *Cu-Au alloy*

According to the analytical results (Table 2), the alloy corresponds to the calculated formula $Cu_{3.02}(Au_{1.91}Fe_{0.04}Ag_{0.01}Pd_{0.01}Sb_{0.01})_{1.98}$ that approaches the ideal stoichiometry Cu_3Au_2. This formula does not fit the two compositions known in the Cu-Au system, auricupride (ideal Cu_3Au) and tetraauricupride (ideal AuCu), and was initially supposed to be a new mineral species. However, the X-ray data indicate that the Uktus Cu_3Au_2 alloy represents a Cu-rich tetraauricupride. We have obtained reflectance measurements on Cu-rich tetraauricupride using a Zeiss microspectrophotometer and following the procedures described by Criddle *et al.* (1983). The data obtained are listed in Table 3 and illustrated in Fig. 11.

Table 3. Reflectance data for the Cu_3Au_2 alloy (Cu-rich tetraauricupride).

Lambda (nm)	R (%)
400	53.1
420	54.4
440	55.7
460	57.4
470	**58.0**
480	58.7
500	60
520	61.1
540	62.3
546	**62.7**
560	63.8
580	65.8
589	**66.7**
600	67.8
620	69.5
640	71.2
650	**71.9**
660	72.6
680	73.9
700	75.3

Values in bold are those recommended by the IMA Commission on Ore Mineralogy (COM).

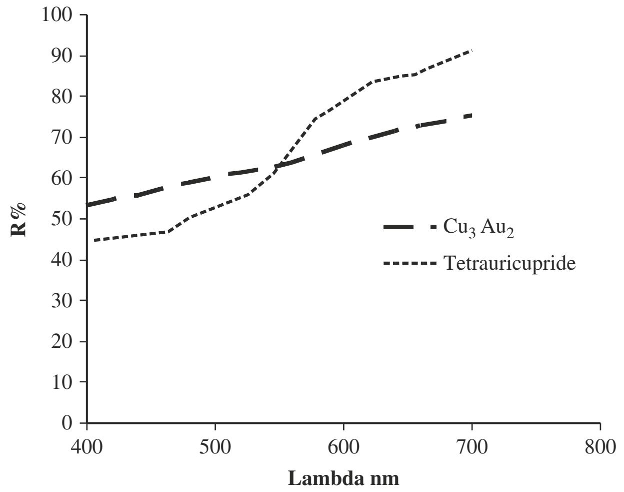

Fig. 11. Spectral reflectance for the Cu_3Au_2 alloy (Cu-rich tetraauricupride) compared with those of tetraauricupride (Keqiao *et al.*, 1982).

5. Discussion

5.1. Possible source of the Uktus nuggets

The mineral assemblage of PGM nuggets can provide useful information concerning their lode deposits. In particular, several papers have demonstrated that Ru-Os-Ir minerals are typical for placers formed by the erosion of ultramafic rocks associated with ophiolite complexes. Alloys in the Pt-Fe-Cu-Ni and Os-Ir-Ru systems are the most abundant nuggets related to the presence of Ural-Alaskan type lode deposits (Razin, 1976; Nixon *et al.,* 1990; Makeyev *et al.,* 1997; Gornostayev *et al.,* 1999; Johan *et al.,* 2000; Tolstykh *et al.*, 2002a and b; Shcheka *et al.*, 2004a, b and c; ; Tolstykh *et al.,* 2004; Barkov *et al.,* 2005, 2008a and b; Johan, 2006; Dill *et al.,* 2010; Fedortchouk *et al.,* 2010). With the exception of the occurrence of tetraauricupride, mineralogical data obtained for the Uktus PGM nuggets are fully consistent with an Ural-Alaskan type source. The mineralogy closely reflects the PGM assemblage previously reported from the Uktus chromitite and dunite (Garuti *et al.,* 2002, 2003) indicating these rocks as the most likely source of the PGM nuggets (Table 4).

5.2. Origin of the Uktus nuggets

5.2.1. *Genetic models for the PGM nuggets in placer deposits*

The origin of PGM nuggets is controversial, with two major proposed models for their formation. One involves primary crystallization of PGM at high magmatic temperature as part of the dunite-chromitite event, followed by their mechanical liberation from the host rocks, transport as suspended particles and concentration in eluvial-alluvial sediments (*e.g.* Cabri *et al.,* 1996). The other suggests that magmatic PGM can be altered during weathering of the

Table 4. Identified PGM in the Uktus complex.

PGM	Chromitites	Nuggets
Pt-Fe alloys	X	X
Tulameenite	x	x
Osmium	X	X
Iridium	X	X
Irarsite	X	X
Hollingworthite		x
Platarsite		x
Laurite	x	x
Erlichmanite	x	
Kashinite	x	x
Cuproiridsite	x	x
Cuprorhodsite	x	
Malanite	x	
Cooperite	x	
Tolovkite	x	x
Potarite	x	
Geversite	x	
Others	x	

X = abundant, x = scarce.

source rocks, the process implying mobility of PGE and transport in aqueous solution, followed by re-deposition, mainly controlled by the Eh-pH conditions, and eventual growth of PGM nuggets in the supergene environment (*e.g.* Bowles, 1986; Bowles *et al.,* 2000). Experiments and the study of natural occurrences indicate that Pd and Pt are particularly mobile in acid soil and in extremely acid or high-chloride waters, travelling as bisulfide or chloride complexes (Fuchs & Rose, 1974; Pan & Wood, 1994; Talovina & Lazarenkov, 2001). However, even the refractory IPGE (Os-Ir-Ru) can be mobilised under hydrothermal or lateritic weathering conditions, sometimes producing secondary PGE alloys, sulfides, sulfarsenides or oxides by alteration of magmatic PGM precursors (*e.g.* Stockman & Hlava, 1984; Garuti & Zaccarini, 1997; Zaccarini *et al.,* 2005; Garuti *et al.,* 2007, 2012).

The Uktus placer deposits show the coexistence of two types of nuggets: (i) nuggets with preserved primary magmatic mineral assemblages and internal textures, and (ii) nuggets showing evidence of low-temperature alteration or secondary reworking and growth at low temperature.

5.2.2. Primary magmatic PGM nuggets

The presence of faceted morphologies in some of the investigated nuggets suggests that these grains were only mechanically liberated and transported for a relatively short distance from their lode deposits. Most of the nuggets are Ir-Os and Pt-Fe-Cu alloys showing conspicuous core–rim zoning. In some cases, the zoning may represent a primary magmatic feature due to variations of the relative activities of the PGM in the system. The zoned osmium (Fig. 4B) may indicate variation of the Ir/Os ratio during primary precipitation of the PGM at magmatic temperature. The native iridium with a small rod-shaped inclusion of laurite (Fig. 5D) probably represents a primary magmatic assemblage preserved at the core of an eroded nugget. In other cases, the interpretation is not obvious. Some nuggets are mainly composed of irarsite containing small spots of osmium (Fig. 5B), or irarsite rimmed with tolovkite (Fig. 5C). The paragenetic assemblages suggest that osmium blebs may represent a post-magmatic exsolution product from an originally Os-rich irarsite. The tolovkite rim indicates a late crystallization of this mineral after irarsite, possibly due to an increase of Sb activity at the expense of S and As, with decreasing temperature. On the other hand, the general structure of the grains does not exclude possible reworking under the action of fluids, in a post-magmatic stage at relatively low temperature.

5.2.3. Altered and secondary PGM nuggets

Several nuggets display well developed porous rims accompanied by chemical changes that can hardly be explained by magmatic processes. The iridium grain in Fig. 4A displays a compact internal core with patches enriched in Pt or in Ru, respectively, possibly representing a primary magmatic zoning. In contrast, the outer rim is intensively pitted with pores and contains dark grey patches enriched in Fe. These features are possibly due to a late chemical corrosion of the primary alloy by reaction with low-temperature fluids, involving partial dissolution of PGE and replacement by Fe. The nugget in Fig. 5A exhibits porous rims enriched in Cu, approaching the composition of tetraferroplatinum developed on a compact core of isoferroplatinum-type alloy with osmium lamellae. This type of association was already observed in PGM from the load chromitite deposits of Uktus (Garuti *et al.,* 2002, 2003) and interpreted as a result of reaction of isoferroplatinum with hydrothermal (?) fluids causing mobilisation of Pt and introduction of Cu, Fe, and Ni (Garuti *et al.,* 2002, 2003). The model implies that the alteration processes started *in situ*, during incipient alteration of the host rock. The altered and new-formed PGM were subsequently liberated from their country rocks, and possibly re-worked in the placer environment, as proposed for PGM nuggets associated with alteration soils and laterites (Fuchs & Rose, 1974; Bowles, 1986; Talovina & Lazarenkov, 2001; Garuti *et al.,* 2012b).

5.2.4. Origin of the quartz–tetraauricupride–PGM nugget

The origin of a composite nugget showing the intimate association of tetraauricupride (Cu_3Au_2) with tulameenite accompanied by hollingworthite, platarsite, and intergrown with quartz (Figs. 6 and 7) is puzzling. Gold minerals and quartz have never been found in the Uktus lode mineralization associated with the chromitite-dunite assemblage, and therefore the provenance of this nugget remains enigmatic. A possible explanation is that the nugget was derived from washing of the laterite cover of the Uktus dunite, thus implying that PGE and Au were mobilised and re-precipitated together with some silica during formation of laterite from the ultramafics. Of course this model requires further investigation.

5.2.5. Implications for a better definition of phase relations in the Cu-Au system

The naturally occurring members of the Cu-Au system, listed with decreasing Au content, are: (1) pure gold, Au, with an $Fm\overline{3}m$ structure and $a = 4.0786$ Å (Batchelder & Simmons, 1965); (2) cuproauride, $CuAu_3$, with a $Pm\overline{3}m$ cubic disordered structure ($a = 3.98$ Å – Kubiak & Janczak, 1991); (3) tetraauricupride, CuAu, with a tetragonal 4/*mmm* structure (distorted derivative of the $Fm\overline{3}m$ structure) and $a = 3.96$, $c = 3.67$ Å (Borelius *et al.,* 1928); (4) auricupride, Cu_3Au, exhibiting either an orthorhombic ordered structure ($a = 3.88$, $b = 42.68$, $c = 3.84$ Å) or a $Pm\overline{3}m$ cubic disordered structure ($a = 3.753$ Å – Borelius *et al.,* 1928); (5) pure copper, Cu, with an $Fm\overline{3}m$ structure and $a = 3.615$ Å (Batchelder & Simmons, 1965). If we consider only the Au contents in the five minerals listed above, we can write that Au100, Au75, Au50, Au25 and Au00 correspond to gold, cuproauride, tetraauricupride, auricupride and copper, respectively. Moreover, a cubic unit-cell parameter can be written for all the five minerals: $a = 4.0786$ Å (Au100), $a = 3.98$ Å (Au75), $a = 3.86$ Å (Au50–obtained by considering a mean of the tetragonal unit-cell parameters), $a = 3.75$ Å (Au25–obtained either by considering a mean of the orthorhombic unit-cell parameters of the substructure or using the parameter of the cubic, primitive lattice) and $a = 3.615$ Å (Au00). The mineral studied here, with a composition Cu_3Au_2 (corresponding to Au40), exhibits a tetragonal 4/*mmm* structure (distorted derivative of the $Fm\overline{3}m$ structure) with $a = 3.91$, $c = 3.62$ Å, and can be considered a Cu-rich tetraauricupride. The cubic lattice parameter that can be written for this mineral is $a = 3.813$ Å. If we plot all the obtained cubic cell parameters and the corresponding Au contents (Fig. 12) an almost perfect linear trend is observed, with the *a* parameter increasing with the increase of Au content according to the following linear equation: a_{pred} (Å) $= 3.625(8) + 0.46(1)$Au (a.p.f.u.). The equation allows determination of the unit-cell parameter directly by the chemical composition, easily obtained by microprobe analysis. For this reason, it can be very useful in the case of lack of precise X-ray data owing to the paucity of samples or intergrowths with other minerals, a very frequent case shown by these minerals.

6. Summary and conclusion

The mineralogical study of nuggets recovered from placer deposits within the Uktus Ural-Alaskan type complex indicates predominance of native Ir-Os and alloys in the Pt-Fe-Cu-Ni system, accompanied by minor PGM of the irarsite–hollingworthite–platarsite series, laurite, cuproiridiste, kashinite and tolovkite. One alloy corresponding to Cu-rich tetraauricupride (Cu_3Au_2) was also found, associated with PGM and quartz. Based on mineralogical analogy it is proposed that the PGE in the nuggets were mostly derived by erosion and chemical leaching of upstream, PGM-bearing chromitite and dunite, located in the hilltops of the Uktus complex, with a possible minor contribution from the laterite cover.

The Uktus occurrence indicates that the nuggets are mostly composed of detrital PGM of primary magmatic origin, mechanically extracted from the lode rock and accumulated in eluvial-alluvial sediments. There is evidence, however, that the primary PGM have become unstable during incipient alteration of the host rock or within the sedimentary environment.

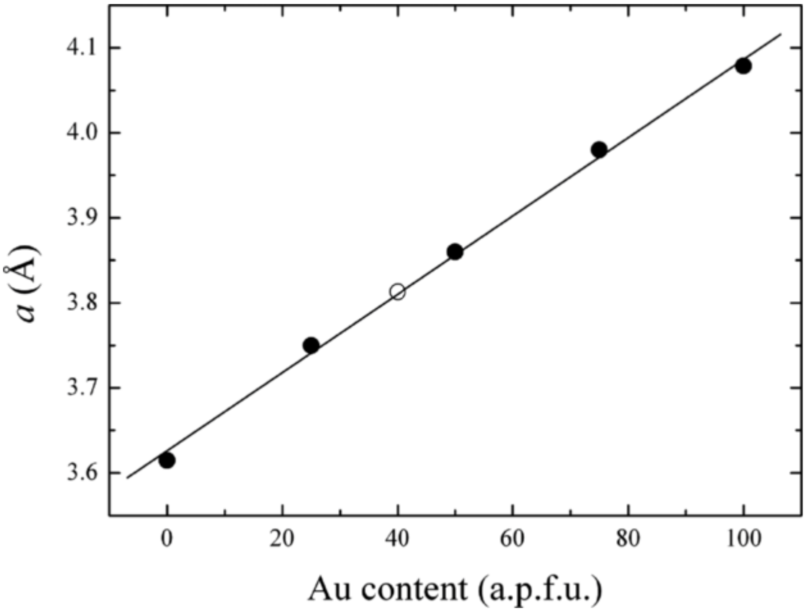

Fig. 12. The cubic cell parameter plotted against Au content in the minerals of the system Cu-Au. Filled symbols refer to data from literature, open symbol to the mineral studied here. The linear regression ($R^2 = 0.997$) is indicated.

The discovery of a Cu-rich tetraauricupride phase allowed better definition of phase relations in the Cu-Au system. Moreover, we emphasize the importance of the crystal-structure investigations of these kind of minerals. In spite of the precise stoichiometry, indeed, like that observed in the mineral studied here (Cu_3Au_2), it was shown that it does not represent a new mineral species, but it is part of the solid solution.

The mineralogical assemblage of the Uktus PGM nuggets, the fact that the Uktus PGM placers have never been mined and the recent exponential increase in noble metals demand make the placers deposits associated with the Uktus complex potentially important for the economic recovery of these rare metals, at least on a small scale.

Acknowledgements: The University Centrum for Applied Geosciences (UCAG) is thanked for the access to the Eugen F. Stumpfl electron microprobe Laboratory. The study of the Russian authors was supported by the grants 12-5-008-NDR and 12--5-1004. The comments of an anonymous referee and N. Tolstykh greatly improved the quality of the manuscript. Many thanks are also due to P. Lattanzi, S. Conticelli and C. Chopin for their editorial handling.

References

Barkov, A.Y., Fleet, M.E., Nixon, G.T., Levson, V.M. (2005): Platinum-group minerals from five placer deposits in British Columbia, Canada. *Can. Mineral.*, **43**, 1687–1710.

Barkov, A.Y., Martin, R.F., LeBarge, W., Fedortchouk, Y. (2008a): Grains of Pt-Fe alloy and inclusions in a Pt-Fe alloy from Florence creek, Yukon, Canada: evidence for mobility of Os in a Na-H_2O-Cl-rich fluid. *Can. Mineral.*, **46**, 343–360.

Barkov, A.Y., Martin, R.F., Shi, L., Feinglos, M.N. (2008b): New data on PGE alloy minerals from a very old collection (probably 1890s), California. *Am. Mineral.*, **93**, 1574–1580.

Batchelder, D.N. & Simmons, R.O. (1965): X-Ray lattice constant of crystals by a rotating-camera method: Al, Ar, Au, CaF_2, Cu, Ge, Ne, Si. *J. Appl. Phys.*, **9**, 2864–2868.

Borelius, G., Johansson, C.H., Linde, J.O. (1928): Die Gitterstrukturumwandlungen in metallischen Mischkristallen. *Ann. Phys.*, **391**, 291–318.

Bowles, J.F.W. (1986): The development of Platinum-Group Minerals in laterite. *Econ. Geol.*, **81**, 1278–1285.

Bowles, J.F.W., Lyon, J.C., Saxton, J.M., Vaughan, D.J. (2000): The origin of Platinum Group Minerals from the Freetown intrusions, Sierra Leone, inferred from osmium isotope systematics. *Econ. Geol.*, **95**, 539–548.

Cabri, L.J. & Genkin, A.D. (1991): Re-examination of Pt alloys from lode and placer deposits, Urals. *Can. Mineral.*, **29**, 419–425.

Cabri, L.J., Harris, D.C., Weiser, T.W. (1996): Mineralogy and distribution of platinum-group mineral (PGM) placer deposits of the world. *Exploration Mining Geol.*, **5**, 73–167.

Cawthorn, R.G. (1999): The platinum and palladium resource of the Bushveld complex. *S. Afr. J. Sci.*, **95**, 481–489.

Criddle, A.J., Stanley, C.J., Chisholm, J.E., Fejer, E.E. (1983): Henryite, a new copper.silver telluride from Bisbee, Arizona. *Bull. Minéral.*, **106**, 511–517.

Dill, H.G., Weber, B., Steyer, G. (2010): Morphological studies of PGM grains in alluvial-fluvial placer deposits from the Bayerischer Wald, SE Germany: hollingworthite and ferroan platinum. *Neues Jb. Miner. Abh.* **187**, 101–110.

Duparc, L. & Tikonowitch, M.N. (1920): Le platine et les gîtes platinifères de l'Oural et du monde. *Soc. Anon. Éd. Son., Rue du Stand*, **46**, Genève, 546 p.

Fedortchouk, Y., LeBarge, W., Barkov, A.Y., Fedele, L., Bodnar, R.J., Martin, R.F. (2010): Platinum group minerals from a placer deposit in Burwash Creek, Kluane area, Yukon Territory, Canada. *Can. Mineral.*, **48**, 583–596.

Fershtater, G.B., Bea, F., Borodina, N.S., Montero, M.P., Smirnov, V.N., Pushkarev, E.V., Rappaport, M.S., Zinger, T.F. (1997): Magmatism as a key to the deep Urals. *Tectonophysics*, **276**, 87–102.

Fuchs, A.W. & Rose, A.W. (1974): The geochemical behavior of platinum and palladium in the weathering cycle in the Stillwater Complex, Montana. *Econ. Geol.*, **69**, 332–346.

Garuti, G. & Zaccarini, F. (1997): In-situ alteration of platinum-group minerals at low temperature: evidence from chromitites of the Vourinos complex (Greece). *Can. Mineral.*, **35**, 611–626.

Garuti, G., Pushkarev, E.V., Zaccarini, F. (2002): Composition and paragenesis of Pt alloys from chromitites of the Uralian-Alaskan-type Kytlym and Uktus complexes, northern and central Urals, Russia. *Can. Mineral.*, **40**, 1127–1146.

Garuti, G., Pushkarev, E.V., Zaccarini, F., Cabella, R., Anikina, E. (2003): Chromite composition and platinum-group mineral assemblage in the Uktus Uralian-Alaskan-type complex (Central Urals, Russia. *Mineral. Deposit.*, **38**, 312–326.

Garuti, G., Proenza, J.A., Zaccarini, F. (2007): Distribution and mineralogy of platinum-group elements in altered chromitites of the Campo Formoso layered intrusion (Bahia State, Brazil): control by magmatic and hydrothermal processes. *Mineral. Petrol*, **86**, 159–188.

Garuti, G., Pushkarev, E.V., Thalhammer, O.A.R., Zaccarini, F. (2012a): Chromite of the Urals (Part 1): overview of chromite mineral chemistry and geo-tectonic setting. *Ofioliti*, **37**, 27–53.

Garuti, G., Zaccarini, F., Proenza, J.A., Thalhammer, O.A.R., Angeli, N. (2012b): Platinum-group minerals in chromitites of the Niquelândia layered intrusion (Central Goias, Brazil): Their magmatic origin and low-temperature reworking during serpentinization and lateritic weathering. *Minerals*, **2**, 365–384.

Gornostayev, S.S., Crocket, J.H., Mochalov, A.G., Laajoki, K.V.O. (1999): The platinum group minerals of the Baimka placer deposits, Aluchin Horst, Russian Far East. *Can. Mineral.*, **37**, 1117–1129.

Harris, D.C. & Cabri, L.J. (1973): The nomenclature of the natural alloys of osmium, iridium and ruthenium based on new compositional data of alloys from world-wide occurrences. *Can. Mineral.*, **12**, 104–112.

Johan, Z. (2006): Platinum nuggets from placers related to the Nizhni Tagil (Middle Urals, Russia) Uralian-Alaskan-type ultramafic complex: ore-mineralogy and study of silicate inclusions in (Pt, Fe) alloys. *Mineral. Petrol*, **87**, 1–30.

Johan, Z., Slansky, E., Kelly, D.A. (2000): Platinum nuggets from the Kompiam area, Enga Province, Papua New Guinea: evidence for an Alaskan-type complex. *Mineral. Petrol*, **68**, 159–176.

Keqiao, C., Tinggao, Y., Yonnge, Z., Zhizhong, P. (1982): Tetra-auricupride, CuAu, discovered in China. *Sci. Geol. Sinica,* **1**, 111–116. (in Chinese with English abstract).

Kubiak, R. & Janczak, J. (1991): X-ray study of ordered phase formation in $Au_{31.6}Cu_{68.4}$, $Au_{50}Cu_{50}$ and $Au_{75}Cu_{25}$. *J. Alloys Comp.*, **176**, 133–140.

Makeyev, A.B., Kononkova, N.N., Kraplya, E.A., Chernukha, F.P., Bryanchaninova, N.I. (1997): Platinum Group Minerals in alluvium of the Northern Urals and Timan: the key to primary sources of platinum. *Trans. Russ. Acad. Sci. Earth Sci. Sect.*, **353**, 181–184.

Mudd, G.M. (2012): Key trends in the resource sustainability of platinum group elements. *Ore Geol. Rev.*, **46**, 106–117.

Nixon, G.T., Cabri, L.J., Gilles Laflamme, J.H. (1990): Platinum group element mineralization in lode and placer deposits associated with the Tulameen Alaskan-type complex, British Columbia. *Can. Mineral.*, **28**, 503–535.

Pan, P. & Wood, S.A. (1994): Solubility of Pt and Pd sulfides and Au metal in aqueous bisulfide solutions. *Mineral. Deposit.*, **29**, 312–326.

Pushkarev, E.V. (2000): Petrology of the Uktus dunite-clinopyroxenite-gabbro massif (the Middle Urals). Monogr. Russian Acad. Sci. Ural Branch, Inst. Geol. Geochem., Ekateriburg, 296 p. (in Russian).

Pushkarev, E.V. & Puchkova, A.V. (1991) The Uktus mafic-ultramafic massif (Middle Urals). In: Geology and Geochemistry. Ural Branch RAS Year Book 1990, Sverdlovsk, 35–37. (in Russian).

Pushkarev, E.V., Gulayeva, T.Y., Palgueva, G.V., Petrisheva, V.G., Sherstobitova, D.A. (1994): The dunites of the Uktus massif. In: Geology and Geochemistry. Ural Branch RAS Year Book 1993, Sverdlovsk, 73–79. (in Russian).

Pushkarev, E.V., Anikina, Ye.V., Garuti, G., Zaccarini, F., Cabella, R. (1999): Geikielite (Mg-ilmenite) in association with Cr-spinel and platinoids from the Uktus massif dunite, Middle Urals: genetic implications. *Dokl. Earth Sci.*, **369A 9**, 1220–1223.

Razin, L.V. (1976): Geologic and genetic features of forsterite dunites and their platinum-group mineralization. *Econ. Geol.*, **71**, 1371–1376.

Shcheka, G.G., Lehmann, B., Gierth, E., Gomann, K., Wallianos, A. (2004a): Macrocrystals of Pt-Fe alloy from the Kondyor PGE placer deposit, Khabarovskiy Kray, Russia: trace-elements content, mineral inclusions and reaction assemblage. *Can. Mineral.*, **42**, 601–517.

Shcheka, G.G., Solianik, A.N., Lehmann, B., Bienok, A., Tolstykh, N.D., Amthauer, G., Topa, D., Laflamme, J.H.G. (2004b): Euhedral crystal of ferroan platinum, cooperite, and mertieite-II from alluvial sediments of the Darya river, Aldan Shield, Russia. *Mineral. Mag.*, **68**, 871–885.

Shcheka, G.G., Vrzhosek, A.A., Lehmann, B., Tolstykh, N.D. (2004c): Association of platinum group minerals from the Zolotaya gold placer, Primorye, Russian Far East. *Can. Mineral.*, **42**, 583–599.

Stockman, H.W. & Hlava, P.F. (1984): Platinum-group minerals in Alpine chromitites from south-western Oregon. *Econ. Geol.*, **79**, 491–508.

Talovina, I.V. & Lazarenkov, V.G. (2001): Distribution and genesis of Platinum group minerals in Nickel Ores of the Sakhara and Elizavet deposits in the urals. *Lithol. Mineral Res.*, **36**, 116–122.

Tokarev, I.F. (1922): The dunite-pyroxenite massif of the Uktus mountains (The petrography of Ekaterinburg neighbourhood). *Notes Uralian Soc. Nature Lovers*, **38**, 1–11. (in Russian).

Tolstykh, N.D., Foley, J.Y., Sidorov, E.G., Laajoki, K.V.O. (2002a): Composition of platinum group minerals in the Salmon river placer deposit, Goodnews Bay, Alaska. *Can. Mineral.*, **40**, 463–471.

Tolstykh, N.D., Krivenko, A., Sidorov, E., Laajoki, K., Podlipsky, M. (2002b): Ore mineralogy of PGM placers in Siberia and the Russian Far East. *Ore Geol. Rev.*, **20**, 1–25.

Tolstykh, N.D., Sidorov, E.G., Kozlov, A.P. (2004): Platinum group element mineralization in lode and placer deposits associated with the Ural-Alaskan-type Galmoenan complex, Koryak-Kamchatka Platinum belt, Russia. *Can. Mineral.*, **42**, 619–630.

Yefimov, A.A., Yefimova, L.P., Maegov, V.I. (1993): The tectonics of the platinum-bearing belt of the Urals: composition and mechanism of structural developments. *Geotectonics*, **27**, 197–207.

Zaccarini, F., Proenza, J.A., Ortega-Gutierrez, F., Garuti, G. (2005): Platinum Group Minerals in ophiolitic chromitites from Tehuitzingo (Acatlan Complex, Southern Mexico): implications for postmagmatic modification. *Mineral. Petrol*, **84**, 147–168.

Zaccarini, F., Pushvarev, E., Dvornik, G.P., Garuti, G., Bigi, S. (2007): Platinum-Group Minerals (PGM) from lode an placers deposits from the Uktus concentrically-zoned complex (Central Urals, Russia). *in* ''Digging deeper, proceedings of the ninth biennial SGA meeting, Dublin 2007'', C.J. Andrew *et al*., eds., 2, 1603–1606.

Received 30 October 2012
Modified version received 11 January 2013
Accepted 25 March 2013